

# Multi Band Cactus Shaped Monopole MIMO Antenna for Wireless LAN and X Band Satellite Communication Applications



Jayshri Kulkarni, Shailesh Kulkarni, and Chow-Yen-Desmond Sim

**Abstract** In this research work, T-Shaped Monopole (TSM) Multiple input multiple output (MIMO) antenna with connected ground is designed and analyzed for wireless local area network (WLAN) and X-band satellite communication applications concurrently. Each TSM applied for MIMO configuration, consists of T-shaped as a main radiator which further is branched into two asymmetrical inverted-F shaped radiators on each side forming a cactus shaped structure and a partial ground plane to achieve impedance matching characteristics. The cactus shaped MIMO antenna is excited by  $50 \Omega$  microstrip feed line to induce two resonances at 5.20 GHz in lower frequency ( $F_L$ ) band and 9.70 GHz in upper frequency ( $F_U$ ) band. Further analysis confirms that fractional impedance bandwidth (FIB) of 10.60% (4.90–5.45 GHz) and 27.80% (8.72–11.55 GHz) are achieved in  $F_L$  and  $F_U$  band, respectively with minimum mutual coupling of  $-20$  dB, gain 3 dBi and efficiency of 65% in both the desired operating bands. Moreover, the MIMO diversity parameters are also analysed for the validation of MIMO applicability.

**Keywords** Monopole antenna · WLAN · X-band · MIMO · And microstrip feed line

## 1 Introduction

In the presence of global pandemic COVID 19, MIMO technologies incorporating multiband antennas plays a very significant role to implement the concept of “Learn

---

J. Kulkarni · S. Kulkarni (✉) · C.-Y.-D. Sim

Department of Electronics and Telecommunication Engineering, Vishwakarma Institute of Information Technology, Pune, India  
e-mail: [Shailesh.kulkarni@viit.ac.in](mailto:Shailesh.kulkarni@viit.ac.in)

J. Kulkarni

e-mail: [Jayashri.kulkarni@viit.ac.in](mailto:Jayashri.kulkarni@viit.ac.in)

C.-Y.-D. Sim

e-mail: [cysim@fcu.edu.tw](mailto:cysim@fcu.edu.tw)

Department of Electrical Engineering, Feng Chia University, Taichung, Taiwan

from home” and “work from home”. Therefore, with the support of MIMO technology, this paper presents the design and analysis of two port cactus shaped MIMO antenna for wireless and satellite communication applications. Recently, a lot outstanding research efforts have been bestowed on the development of single/multiband/MIMO antenna [1–10].

A MIMO antenna incorporating two antenna array elements operating in X-band is revealed in [1]. An electronic band gap (EBG) structure is utilized to realize high isolation upto  $-22$  dB in the working band of (8.00–12.00 GHz). However, the MIMO antenna possess the size of  $55 \times 49$  mm<sup>2</sup> and is printed on FR-4 substrate having thickness of 1.6 mm. However, the EBG structure always require a size greater than  $0.1\lambda$ , which makes the structure complicated in practical implementation. This in turn affects the radiation features of the complete wireless devices. In order to reduce the size of antenna array as well as complexity and also to operate the antenna array in X band similar to [1], a microstrip fed patch antenna with the size of  $43 \times 43$  mm<sup>2</sup> is described in [2]. The described antenna is printed on expensive Rogers RT duroid 5880 substrate having thickness of 1.27 mm. However, while forming MIMO configuration, the antenna elements need to be closely packed with the conductive elements which leads in deteriorating the performance of MIMO antenna. Apart from the above, the antennas reported in [1–2] operate in single band only. An orthogonally placed, two port microstrip fed MIMO antenna operating in WLAN/INSAT/Super extended-C band is revealed in [3]. Here, in this antenna a parasitic rectangular strip and slots are inserted in the ground which helps to improve isolation upto 16 dB. Further, an orthogonal arrangement of antenna elements radiates orthogonally with each other which results in reduction of mutual coupling of antenna elements. A two element MIMO antenna working in (6.30–12.50 GHz) covering entire X-band application is reported in [4]. In this antenna an air gap in the radiator of antenna element is introduced which offer minimum isolation of  $-35$  dB in the functioning band. However, MIMO antenna has footprint of  $66 \times 23$  mm<sup>2</sup> and is engraved on expensive 3.2 mm thick RT duroid substrate. To minimize the fabrication cost of the antenna, a four port MIMO antenna with minimum isolation of  $-20$  dB for simultaneous functioning in entire sub 6 GHz and WLAN band is reported in [5]. The size of reported antenna is  $30 \times 40$  mm<sup>2</sup> and designed on cost effective FR-4 substrate of 1.6 mm.

To accommodate the advantages of coplanar waveguide (CPW) fed technique, a two port MIMO antenna covering the bandwidth of sub-6 GHz/Wi-Fi-5/V2X/DSRC/Wi-Fi-6/INSAT-C is reported in [6]. The reported MIMO antenna uses FR-4 substrate and has designed volume of  $32 \times 22 \times 0.8$  mm<sup>3</sup>. A triple band microstrip fed arc shaped antenna with inverted L-shaped stubs is communicated in [7]. The reported antenna operates in WLAN (2.48–2.4835, 5.15–5.875 GHz) and X-band (7.25–7.75 GHz) for wireless and satellite communication applications. However, the reported antenna is effective to partial bandwidth requirement of X-band. In order to cover the entire bandwidth of X-band, a coaxial fed S-shaped patch antenna is reported in [8]. The size of antenna is  $20 \times 17.2$  mm<sup>2</sup> and is built on economical 1.6 mm FR-4 substrate. However, the prob feeding technique may

result in fabrication difficulty and spurious radiation. A multiband and compact flexible ultra-wide band (UWB) antenna and CPW fed antennas are reported in [9–10]. However, the antenna [9–10] are single antenna element and does not provide high data rates and low latency.

In this manuscript, a dual band cactus shaped monopole MIMO antenna with connected ground and high isolation for wireless and satellite communication applications is proposed. This cactus shaped MIMO antenna consists of two antenna elements with a minimum footprint of  $30 \times 30 \text{ mm}^2$  for each element. To reduce a mutual coupling between the cactus shaped antennas, two symmetrical inverted U-shaped structure are introduced from ground planes. The proposed cactus shaped MIMO antenna is designed, analyzed and simulated using CST software to operate in  $F_L$  (4.90–5.45 GHz) and  $F_U$  (8.72–11.55 GHz) with minimum isolation of  $-20 \text{ dB}$ .

The manuscript is arranged as follows: Sect. 2 illustrates the layout and evolution mechanism of single cactus shaped antenna, Sect. 3 explains the MIMO geometry with decoupling structure, Sect. 4 gives insights on results and discussion. To prove the novelty and contribution, a performance comparison is presented in Sect. 5 and finally, paper is concluded in Sect. 6.

## 2 Layout and Evolution Mechanism of Cactus Shaped Antenna

The simplified design layout of single monopole antenna is depicted in Fig. 1 for wireless and satellite communication operation. The proposed antenna consists of

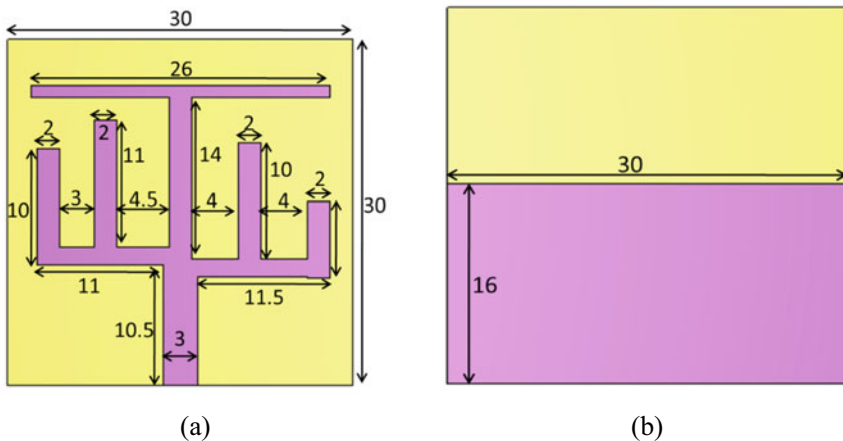


**Fig. 1** Geometry and layout of proposed cactus shaped antenna (all dimensions in mm) **a** Front view **b** Back view

T-shaped main radiator which is further branched into two asymmetrical inverted-F shaped radiators on each side, forming a cactus shaped structure and a partial ground plane to achieve impedance matching characteristics. The proposed single cactus shaped antenna is designed on FR-4 substrate having a size of  $30 \times 30 \text{ mm}^2$  (thickness 0.8 mm, loss tangent 0.025 and dielectric permittivity of 4.3).

## 2.1 Evolution Mechanism of Proposed Cactus Shaped Antenna

The evolution mechanism of proposed cactus shaped antenna is illustrated in Fig. 2. For analyzing the operating mechanism of proposed cactus shaped antenna, the reflection coefficient curve ( $S_{11}$ ) dB of each step is depicted in Fig. 2. Initially, to achieve bandwidth of X-band ( $F_U$ ) band, a feed line with an inverted F-shape structure on right side as shown in Fig. 2 is excited by  $50 \Omega$  microstrip feeding line. Due to proper impedance matching and accurate feeding arrangement, the step-1 is able to induce a resonance at (10.70–11.30 GHz) which can be easily noted from Fig. 2. However, the induced bandwidth is very less. Therefore, in order to enhance the impedance bandwidth of setp-1, a step-2 is developed where, another inverted-F shaped structure to left of step-1 is branched out without disturbing the feeding position as shown in Fig. 2b. The corresponding  $S_{11}$  curve of step-2 is shown in Fig. 2. It is noted that the step-2 is able to enhance bandwidth in the frequency range of (8.72–11.55 GHz)

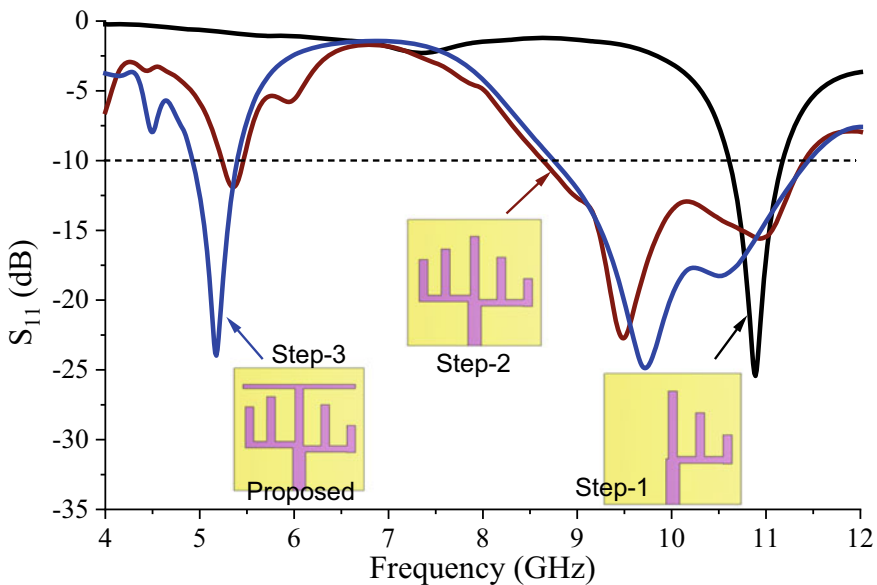


Fig. 2 Step wise design of proposed antenna

because the elongation of current path flowing through all radiator for longer time. The step-2 antenna could operate in  $F_U$  band with frequency range of (8.72–11.55 GHz), conforming the bandwidth need of X-band.

Further, to have another resonance at 5.2 GHz, a horizontal strip is added on top of the vertical strip extended from feedline forming a T-shape structure. The length of T-shaped radiator to resonate at required frequency is calculated by using below Eq. (1)

$$\lambda = \frac{C}{\sqrt{\epsilon_{eff} f}} \tag{1}$$

where in Eq. (1),  $\epsilon_{eff} = \frac{\epsilon_r + 1}{2}$ ,  $\epsilon_r$  is dielectric permittivity of FR-4 substrate and  $C$  is speed of light in  $3 \times 10^8$  m/s.

This structure termed as step-3 helps in inducing a resonance at 5.20 GHz covering a frequency range of (4.90–5.45 GHz) as shown in Fig. 2. Thus, the proposed cactus shaped antenna induces two resonances at 5.20 and 9.70 GHz operating in frequency band of  $F_L$  (4.90–5.45 GHz) and  $F_U$  (8.72–11.55 GHz), respectively as visualized in Fig. 2.

Further, to perceive more about working principal of proposed cactus shape antenna, a surface current distribution (A/m) is analyzed in Fig. 3. From Fig. 3a, it is noted that a more amount of current is flowing through T-radiator, confirming that this structure contributes to induce a resonance at 5.20 GHz with impedance bandwidth of 10.62% (4.80–5.45 GHz). Further, at resonance 9.70 GHz, analyzed from Fig. 3b, more amount of current is flowing through two asymmetrical F-shaped radiators thus inducing an impedance bandwidth of 27.8% (8.72–11.55 GHz).

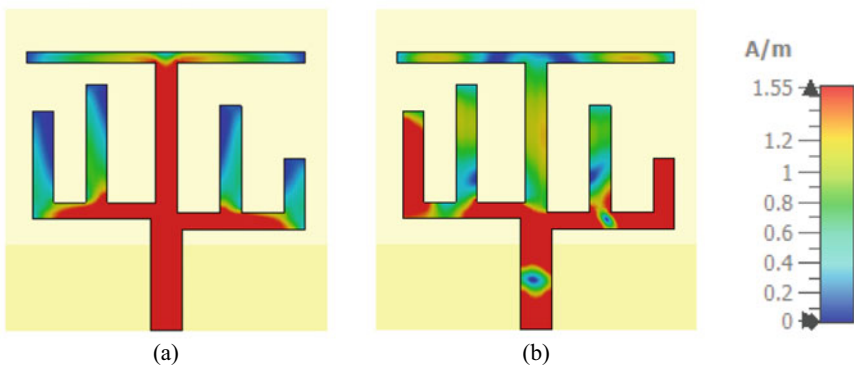
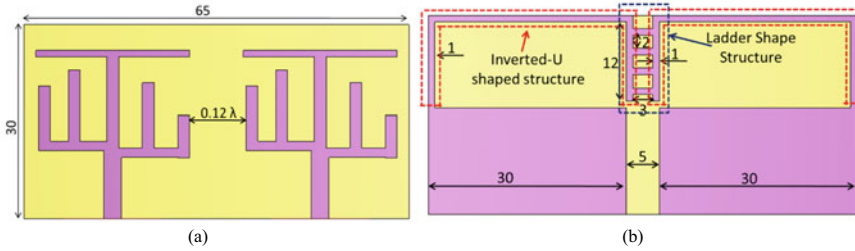


Fig. 3 Surface current distribution of proposed antenna a 5.2 GHz b 9.7 GHz



**Fig. 4** Geometry and layout of proposed TSM MIMO antenna (all dimensions in mm) **a** Front view **b** Back view

### 3 Proposed Cactus Shaped MIMO Antenna Geometry

The proposed cactus shaped MIMO antenna has designed footprint of  $65 \times 30 \text{ mm}^2$  ( $1.12\lambda \times 0.52\lambda$ ) and comprises of two antenna elements located at an edge-to-edge distance of  $0.12\lambda$  (where  $\lambda$  is free space wavelength measured at 5.20 GHz) on top layer of FR-4 substrate as depicted in Fig. 4a. Figure 4b depicts that the bottom layer of FR-4 substrate which basically consists of two partial ground plane, two symmetrical inverted U-shaped structure branched out from the partial ground planes. Further, these two inverted-U shaped structures are connected using 4 horizontal strips of  $1 \times 3 \text{ mm}^2$  each forming a ladder structure at the centre. This structure serves as a decoupling structure to reduce the mutual coupling of antenna elements and also enhances the diversity performance of proposed MIMO antenna.

### 4 Results and Discussion

The proposed cactus shaped MIMO antenna design is validated by comparing the scattering parameters including reflection coefficient curve and transmission coefficient curve. However, due to analogy of  $S_{11}$ – $S_{22}$  and  $S_{12}$ – $S_{21}$ , only  $S_{11}$  and  $S_{12}$  curves are illustrated in Fig. 5. From the Fig. 5, it is visualized that antenna element operates in  $F_L$  and  $F_U$  bands with the same bandwidth as it is achieved in Fig. 2, while the  $S_{12}$  curve shows that the minimum mutual coupling between antenna elements is –20 dB in both the operating bands of  $F_L$  and  $F_U$ .

Moreover, to realize the operating mechanism of decoupling structure, an electric field intensity distribution (V/m) is analyzed in Fig. 6. This analysis is performed under the condition that when one antenna element (port 1) is active, other antenna element (port 2) is matched with  $50 \Omega$  load impedance. From Fig. 6, it is visualized that both the antenna elements remain protected from electric field of each other as amount of current flows through the decoupling structure.

The three-dimensional (3D) and two-dimensional (2D) radiation patterns of the proposed cactus shaped MIMO antenna at 5.20 and 9.70 GHz are depicted in Figs. 7

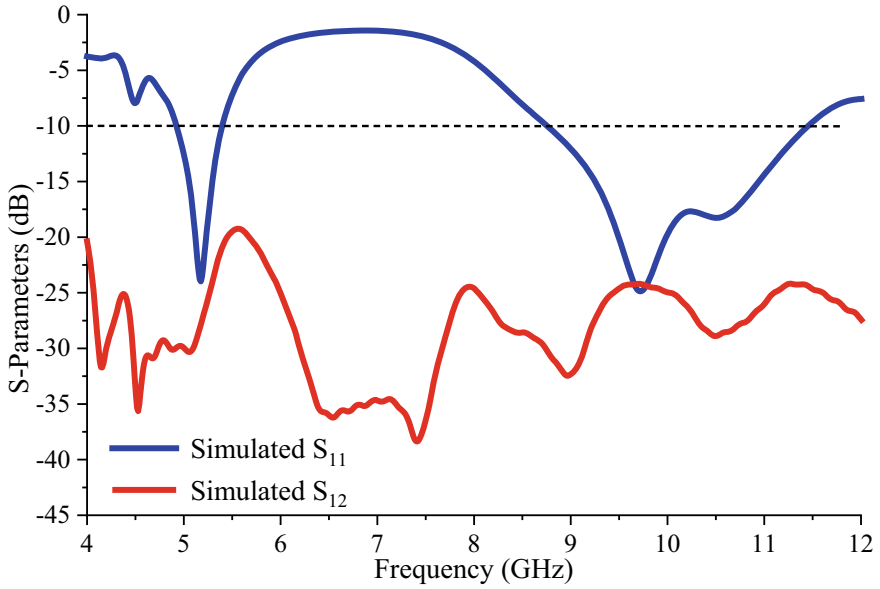


Fig. 5 S-Parameters of proposed MIMO antenna

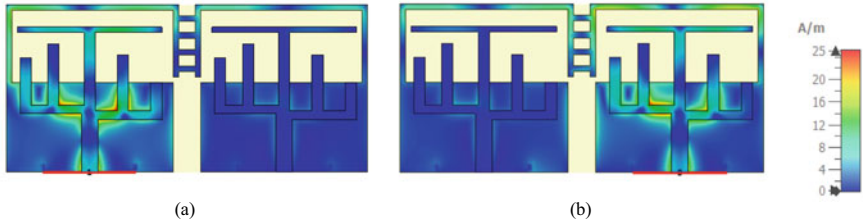


Fig. 6 Electric field intensity distribution (V/m) a When port-1 is excited b when port 2 is excited

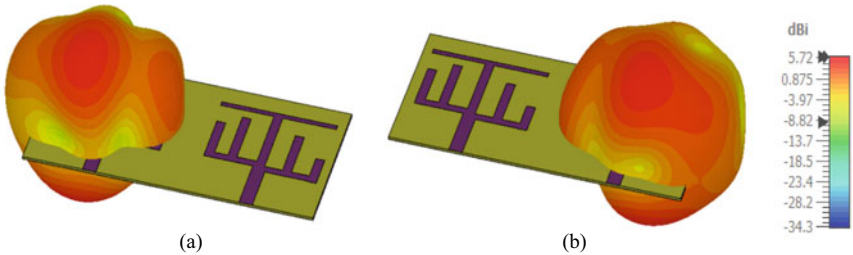
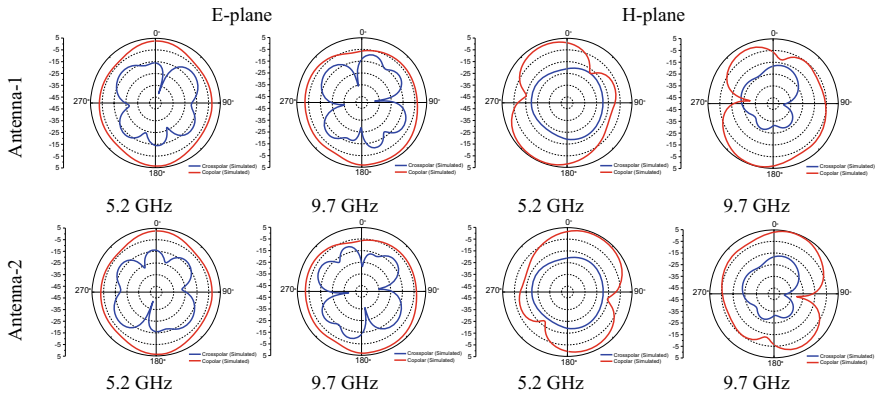


Fig. 7 3D radiation pattern of proposed MIMO antenna a Antenna-1 b Antenna-2



**Fig. 8** 2D radiation pattern of proposed MIMO antenna

and 8, respectively. Both the radiation patterns are matched with each other with negligible nulls and obtained by keeping only one antenna element active, while the other one is terminated with  $50 \Omega$  load impedance. At both the resonances, the radiation patterns are just like a monopole, whose co-polar radiation is an omnidirectional radiation with higher magnitude than cross polar radiation in the plane at the both the resonant frequencies.

The gain and efficiency of the proposed cactus shaped MIMO antenna is shown in Fig. 9(a). The minimum gain is 3.5 dBi at 5.2 GHz and 3 dBi at 9.7 GHz, whereas radiation efficiency is 65% at 5.20 GHz and 70% at 9.70 GHz. The correlation coefficient is an important metric to calculate the diversity performance of proposed cactus shaped MIMO antenna and plotted in Fig. 9(b). From this figure, it is visualized that the ECC of the proposed cactus shaped MIMO antenna is well below 0.05 whereas the DG is well above 9.95 throughout the operating band.

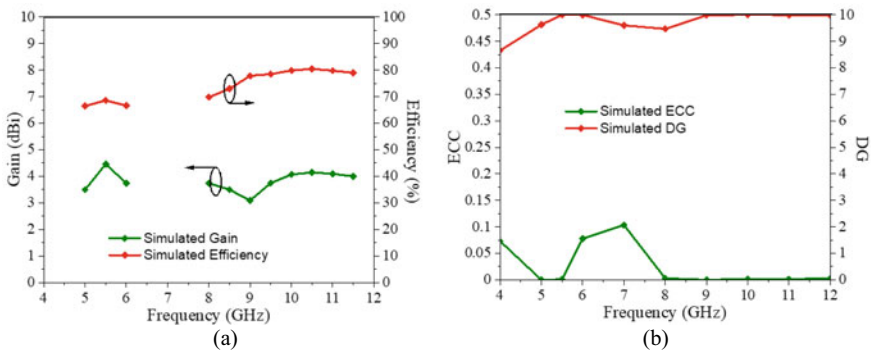


**Fig. 9** a Gain and efficiency b ECC and DG

**Table 1** Performance comparison of proposed cactus shaped MIMO antenna

Ref.	Antenna element	Band (GHz)	Dimension (mm <sup>2</sup> )	Thickness (mm)	Substrate	Gain (dBi)
[1]	Single	8.00–12.00	55 × 49	1.6	FR-4	2.2
[2]	Single	8.00–12.00	43 × 43	1.27	RT-Duroid	7.4
[3]	Two	4.64–9.00	25 × 34.80	1.6	FR-4	4.21
[4]	Two	8.00–12.00	66 × 33	3.2	RT Duroid	6.0
[7]	One	2.28–2.57/ 5.00–6.27/ 7.11–7.96	18 × 34.5	0.8	FR-4	1.0
[8]	Single	8.69–9.14/ 10.47–11.48/ 11.53–11.98	20 × 17.2	1.6	FR-4	2.5
[9]	One	1.33–11.11	35 × 35	0.2	FR-4	3.3
[Proposed]	Two	4.90–5.45/ 8.72–11.55	65 × 30	0.8	FR-4	3.0

## 5 Performance Comparison of Proposed Cactus Shaped MIMO Antenna

For validating the performance of the proposed cactus shaped MIMO antenna, a comparative study is tabulated in Table 1. The parameters considered for performance are no. of antenna elements, operating bands, dimension, thickness, type of substrate used and gain.

The advantages of proposed cactus shaped MIMO antenna are as follows:

1. The proposed MIMO antenna has less dimensions than [4] and cost effective than [2, 4].
2. The proposed MIMO antenna has two antenna elements as compared with all except [3, 4].
3. The proposed MIMO antenna operates in dual band unlike [1, 2, 3] with relatively thin thickness unlike [4].
4. The proposed MIMO antenna exhibit high gain as compared to [1] and [7]

## 6 Conclusion

A cactus shaped monopole MIMO antenna with inverted-U shaped (connected with ladder) as a decoupling structure is presented for WLAN and X-band application. The proposed cactus shaped MIMO antenna with interconnected ground operates at (4.90–5.45 GHz) WLAN and (8.72–11.55 GHz) X-band with minimum isolation of –20 dB. The MIMO antenna also exhibit gain of above 3 dBi, efficiency above 65%, ECC below 0.05 and DG above 9.95 throughout the operating frequency band.

Finally, a comparison between the current state of art and the proposed cactus shaped MIMO antenna is presented. From the comparative study it can be concluded that the proposed cactus shaped MIMO antenna a good contender for WLAN and X band applications.

## References

1. Saxena G, Jain P, Awasthi YK (2019) High isolation EBG based MIMO antenna for X-band applications. In: 2019 6th international conference on signal processing and integrated networks (SPIN), pp 97–100
2. Varghese NM, Vincent S, Kumar OP (2016) Design and analysis of cross-fed rectangular array antenna; an X-band microstrip array antenna, operating at 11 GHz. In: 2016 international conference on advances in computing, communications and informatics (ICACCI), pp 1261–1265
3. Banerjee J et al (2020) An orthogonally oriented multiband MIMO antenna for WLAN, C-band and X-band wireless applications. In: 2020 IEEE Calcutta conference (CALCON), pp 328–332
4. Babu KJ, Kumar BK, Boddu SR, Krishna KSR (2017) Design of a MIMO dielectric resonator antenna with air gap for X-band applications. In: 2017 progress in electromagnetics research symposium - Fall (PIERS - FALL), pp 1835–1838
5. Jayshri K, Arpan D, Sim CYD (2020) Wideband four-port MIMO antenna array with high isolation for future wireless systems. *Int J Electron Commun (AEU)* 128:1–14
6. Kulkarni J, Desai A, Sim C-Y (2021) Two port CPW-fed MIMO antenna with wide bandwidth and high isolation for future wireless applications. *Int J RF Microw Comput Aided Eng* 31:1–16
7. Zhi R, Han M, Bai J, Wu W, Liu G (2018) Miniature multiband antenna for WLAN and X-band satellite communication applications. *Progr Electromagn Res Lett* 75:13–18
8. Samsuzzaman M, Islam MT (2014) Inverted S-shaped compact antenna for X-band applications. *Sci World J* 2014:11
9. Kumar S, Khan T (2018) CPW-fed UWB flexible antenna for GSM/WLAN/X-band applications. In: 2018 5th international conference on signal processing and integrated networks (SPIN), pp 126–129
10. Kulkarni J (2020) Design and analysis of multiband CPW-fed antenna for industrial wireless applications. In: 2020 IEEE 7th Uttar Pradesh section international conference on electrical, electronics and computer engineering (UPCON), pp 1–5